Title
Nutrient Signaling via the TORC1-Greatwall-PP2AB55δ Pathway Responsible for the High Initial Rates of Alcoholic Fermentation in Sake Yeast Strains of Saccharomyces cerevisiae

Journal
Applied and Environmental Microbiology, 85(1)

ISSN
0099-2240

Authors
Watanabe, Daisuke
Kajihara, Takuma
Sugimoto, Yukiko
et al.

Publication Date
2019

DOI
10.1128/aem.02083-18

Peer reviewed

AMERICAN SOCIETY FOR MICROBIOLOGY | Applied and Environmental Microbiology®

FOOD MICROBIOLOGY

Nutrient Signaling via the TORC1-Greatwall-PP2A$^{B55\delta}$ Pathway Is Responsible for the High Initial Rates of Alcoholic Fermentation in Sake Yeast Strains of *Saccharomyces cerevisiae*

Daisuke Watanabe,[a,b] Takuma Kajihara,[a] Yukiko Sugimoto,[a] Kenichi Takagi,[a] Megumi Mizuno,[b] Yan Zhou,[b] Jiawen Chen,[c] Kojiro Takeda,[d,e] Hisashi Tatebe,[a] Kazuhiro Shiozaki,[a] Nobushige Nakazawa,[f] Shingo Izawa,[g] Takeshi Akao,[b] Hitoshi Shimoi,[b,h] Tatsuya Maeda,[c]* Hiroshi Takagi[a]

[a]Division of Biological Science, Graduate School of Science and Technology, Nara Institute of Science and Technology, Ikoma, Nara, Japan
[b]National Research Institute of Brewing, Higashihiroshima, Hiroshima, Japan
[c]Institute of Molecular and Cellular Biosciences, University of Tokyo, Tokyo, Japan
[d]Department of Biology, Faculty of Science and Engineering, Konan University, Kobe, Japan
[e]Institute for Integrative Neurobiology, Konan University, Kobe, Japan
[f]Department of Biotechnology, Faculty of Bioresource Science, Akita Prefectural University, Akita, Akita, Japan
[g]Graduate School of Science and Technology, Kyoto Institute of Technology, Kyoto, Japan
[h]Faculty of Agriculture, Iwate University, Morioka, Iwate, Japan

ABSTRACT *Saccharomyces cerevisiae* sake yeast strain Kyokai no. 7 (K7) and its relatives carry a homozygous loss-of-function mutation in the *RIM15* gene, which encodes a Greatwall family protein kinase. Disruption of *RIM15* in nonsake yeast strains leads to improved alcoholic fermentation, indicating that the defect in Rim15p is associated with the enhanced fermentation performance of sake yeast cells. In order to understand how Rim15p mediates fermentation control, we here focused on target-of-rapamycin protein kinase complex 1 (TORC1) and protein phosphatase 2A with the B55δ regulatory subunit (PP2A$^{B55\delta}$), complexes that are known to act upstream and downstream of Rim15p, respectively. Several lines of evidence, including our previous transcriptomic analysis data, suggested enhanced TORC1 signaling in sake yeast cells during sake fermentation. Fermentation tests of the TORC1-related mutants using a laboratory strain revealed that TORC1 signaling positively regulates the initial fermentation rate in a Rim15p-dependent manner. Deletion of the *CDC55* gene, encoding B55δ, abolished the high fermentation performance of Rim15p-deficient laboratory yeast and sake yeast cells, indicating that PP2A$^{B55\delta}$ mediates the fermentation control by TORC1 and Rim15p. The TORC1-Greatwall-PP2A$^{B55\delta}$ pathway similarly affected the fermentation rate in the fission yeast *Schizosaccharomyces pombe*, strongly suggesting that the evolutionarily conserved pathway governs alcoholic fermentation in yeasts. It is likely that elevated PP2A$^{B55\delta}$ activity accounts for the high fermentation performance of sake yeast cells. Heterozygous loss-of-function mutations in *CDC55* found in K7-related sake strains may indicate that the Rim15p-deficient phenotypes are disadvantageous to cell survival.

IMPORTANCE The biochemical processes and enzymes responsible for glycolysis and alcoholic fermentation by the yeast *S. cerevisiae* have long been the subject of scientific research. Nevertheless, the factors determining fermentation performance *in vivo* are not fully understood. As a result, the industrial breeding of yeast strains has required empirical characterization of fermentation by screening numerous mutants through laborious fermentation tests. To establish a rational and efficient breeding strategy, key regulators of alcoholic fermentation need to be identified. In

Citation Watanabe D, Kajihara T, Sugimoto Y, Takagi K, Mizuno M, Zhou Y, Chen J, Takeda K, Tatebe H, Shiozaki K, Nakazawa N, Izawa S, Akao T, Shimoi H, Maeda T, Takagi H. 2019. Nutrient signaling via the TORC1-Greatwall-PP2A$^{B55\delta}$ pathway is responsible for the high initial rates of alcoholic fermentation in sake yeast strains of *Saccharomyces cerevisiae*. Appl Environ Microbiol 85:e02083-18. https://doi.org/10.1128/AEM.02083-18.

Editor M. Julia Pettinari, University of Buenos Aires

Address correspondence to Daisuke Watanabe, d-watanabe@bs.naist.jp.

* Present address: Tatsuya Maeda, Department of Biology, Hamamatsu University School of Medicine, Hamamatsu, Shizuoka, Japan.

Received 24 August 2018
Accepted 13 October 2018
Accepted manuscript posted online 19 October 2018
Published 13 December 2018

the present study, we focused on how sake yeast strains of *S. cerevisiae* have acquired high alcoholic fermentation performance. Our findings provide a rational molecular basis to design yeast strains with optimal fermentation performance for production of alcoholic beverages and bioethanol. In addition, as the evolutionarily conserved TORC1-Greatwall-PP2A$^{B55\delta}$ pathway plays a major role in the glycolytic control, our work may contribute to research on carbohydrate metabolism in higher eukaryotes.

KEYWORDS Cdc55p, Greatwall, PP2A$^{B55\delta}$, Rim15p, *Saccharomyces cerevisiae*, *Schizosaccharomyces pombe*, TORC1, alcoholic fermentation, sake yeast

Sake, an alcoholic beverage made from fermented rice, typically has a higher alcohol content than beer or wine. During sake fermentation, saccharification by hydrolytic enzymes of *Aspergillus oryzae* and alcoholic fermentation by *Saccharomyces cerevisiae* sake yeast are the major bioconversions. Thus, the high alcohol content of sake is at least partly attributable to the unique characteristics of sake yeast. Sake yeast strains have long been selected based on the high fermentation performance as well as the balanced production of aroma and flavor compounds (1, 2). Our previous comparative genomic and transcriptomic analyses revealed that a representative sake yeast, strain Kyokai no. 7 (K7), and its relatives carry a loss-of-function mutation in *RIM15* (*rim15*$^{5054\_5055insA}$), a gene of a highly conserved Greatwall family protein kinase (3–5). Disruption of the *RIM15* gene in nonsake yeast strains, such as laboratory, beer, and bioethanol strains, leads to an increase in the fermentation rate (5–9), demonstrating that Rim15p inhibits alcoholic fermentation. Thus, the *rim15*$^{5054\_5055insA}$ mutation appears to be associated with the enhanced fermentation property of K7. Nevertheless, this loss-of-function mutation cannot be solely responsible for the sake yeast's improved fermentation, because expression of the functional *RIM15* gene does not suppress alcoholic fermentation in K7 (5). To better understand this phenomenon, the Rim15p-mediated fermentation control needs to be further dissected through comparative analysis between sake and nonsake yeast strains.

While Rim15p has been identified as a key inhibitor of alcoholic fermentation, involvement of the upstream regulators of Rim15p (Fig. 1) in fermentation control has not yet been fully examined. In *S. cerevisiae*, Rim15p activity is under the control of several nutrient-sensing signaling protein kinases, including protein kinase A (PKA), the phosphate-sensing cyclin and cyclin-dependent protein kinase (CDK) complex termed Pho80p-Pho85p, and target-of-rapamycin protein kinase complex 1 (TORC1) (10, 11). Thus, inactivation of these kinases under nutrient starvation or other stress conditions may trigger Rim15p-dependent inhibition of alcoholic fermentation. Activation of TORC1 is mediated by the heterodimeric Rag GTPases (Gtr1p-Gtr2p in *S. cerevisiae*), which are negatively regulated by the Seh1p-associated protein complex inhibiting TORC1 (SEACIT) subcomplex (Iml1p-Npr2p-Npr3p in *S. cerevisiae*), which acts as a GTPase-activating protein for Gtr1p (12–14). Active TORC1 phosphorylates multiple targets, including Sch9p, the yeast orthologue of the mammalian serum and glucocorticoid-regulated kinase (SGK) (15). Direct phosphorylation of Rim15p at Ser1061 by Sch9p contributes to sequestration of Rim15p in the cytoplasm, thereby inhibiting Rim15p functions (16). Recently, it was reported that the TORC1-Sch9p-Rim15p pathway is conserved and present in the evolutionarily distant fission yeast *Schizosaccharomyces pombe* (17), although it remains to be determined if the pathway affects the fermentation performance in this yeast species. In contrast, mammalian TORC1 (mTORC1) positively regulates glycolysis by the induction of glycolytic gene expression through hypoxia-inducible factor 1α (HIF1α) (18).

In *S. cerevisiae*, Rim15p targets the redundant transcription factors Msn2p and Msn4p (Msn2/4p) to mediate entry into the quiescent state (19, 20). In the context of fermentation control, Rim15p and Msn2/4p are required for the transcriptional induction of the UDP-glucose pyrophosphorylase-encoding gene *UGP1*, which switches the mode of glucose metabolism from glycolysis (a catabolic mode) to UDP-glucose

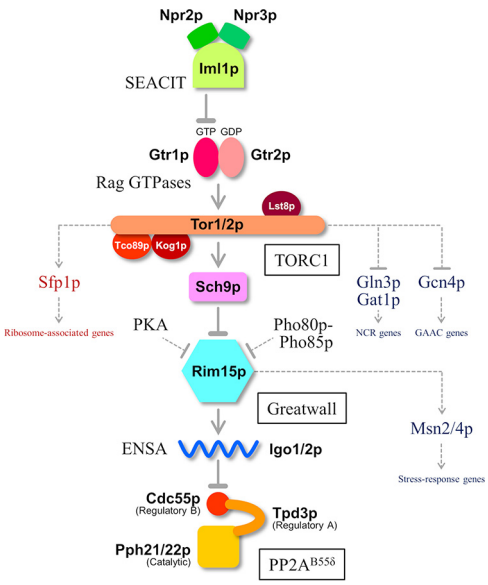

FIG 1 The TORC1-Greatwall-PP2A$^{B55\delta}$ pathway and its associated factors in *S. cerevisiae*. Increased Sfp1p-targeted gene expression and decreased Gln3p-, Gat1p-, Gcn4p-, and Msn2/4p-targeted gene expression were observed in sake yeast cells, suggesting high TORC1 activity. TORC1, target of rapamycin complex 1; PP2A$^{B55\delta}$, protein phosphatase 2A complexed with a regulatory subunit B55δ; SEACIT, Seh1p-associated protein complex inhibiting TORC1; PKA, protein kinase A; NCR, nitrogen catabolite repression; GAAC, general amino acid control.

synthesis (an anabolic mode) (7). However, no orthologue of Msn2/4p has been found in other organisms, and the role of the Greatwall family protein kinases in carbohydrate metabolism is unknown in *S. pombe* or higher eukaryotes. The Greatwall protein kinase was originally identified as a potential cell cycle activator in *Drosophila* (21). In animals, Greatwall directly phosphorylates a small protein called α-endosulfine (ENSA), which inhibits the activity of protein phosphatase 2A accompanied by the regulatory subunit B55δ (PP2A$^{B55\delta}$) (22, 23). Due to the antimitotic activity of PP2A$^{B55\delta}$, Greatwall is required for maintenance of mitosis. More recently, the Greatwall-ENSA-PP2A$^{B55\delta}$ pathway was reported to be conserved in *S. cerevisiae*; Rim15p phosphorylates ENSA orthologues Igo1/2p to inhibit PP2A with the Cdc55p regulatory subunit (24–26). The orthologous pathway has also been found in *S. pombe*, and it plays a pivotal role in TORC1-mediated cell cycle control (17). However, the effect of PP2A$^{B55\delta}$ on fermentation performance was unknown.

In the present study, we tested whether the TORC1-Greatwall-PP2A$^{B55\delta}$ pathway participates in the control of alcoholic fermentation in *S. cerevisiae* and *S. pombe*. Our results provide new insights into how yeast cells determine the mode of glucose metabolism, especially in the context of the enhanced fermentation performance of sake yeast strains.

RESULTS

TORC1-associated transcriptomic profiles during alcoholic fermentation in laboratory and sake yeast strains. Our previous comparative transcriptomic analysis indicated that the expression of the Rim15p- and Msn2/4p-targeted genes was attenuated in K701 (a strain derived from K7) compared to that in the laboratory strain X2180 early in a 20-day sake fermentation test (3). This may be attributed not only to the sake yeast-specific loss-of-function mutation in the *RIM15* gene (*rim15*$^{5054\_5055insA}$; see also reference 5) but also to higher TORC1 activity in the sake strains. TORC1 activity induces the ribosomal genes and the ribosome biogenesis genes, while it represses the general amino acid control (GAAC) and nitrogen catabolite repression (NCR) genes, as well as the Rim15p- and Msn2/4p-dependent stress response genes (27) (Fig. 1). We revisited our previous transcriptomic data indicating that among all differences in gene expres-

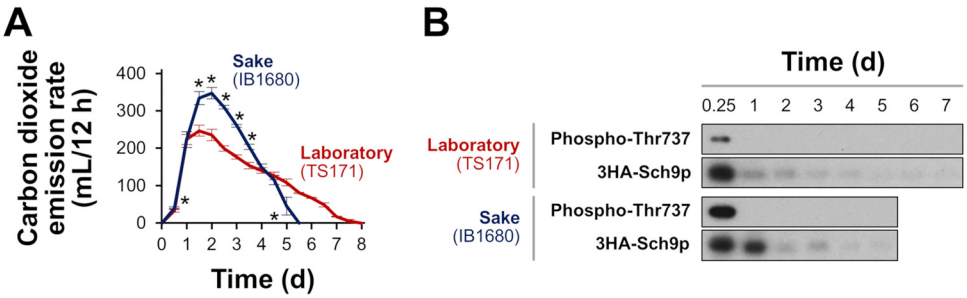

FIG 2 Phosphorylation levels of the Thr737 residue of Sch9p, comparing laboratory and sake strains during an 8-day fermentation test in YPD20. (A) Carbon dioxide emission rates of a laboratory strain (TS171; red) and a sake strain (IB1680; blue). Data represent the mean ± standard deviation (SD) from three (for TS171) or four (for IB1680) independent experiments. *, significant difference (*t* test, $P < 0.05$) compared to the laboratory strain at the respective time point. (B) The phosphorylation status of the Thr737 residue of Sch9 in a laboratory strain (TS171, upper panels) and a sake strain (IB1680, lower panels) was analyzed by Western blotting with an anti-phospho-T737-Sch9 antibody, and the total protein level of 3HA-Sch9p was assayed with an anti-HA antibody, as previously described (28). An equal amount of protein from the whole-cell lysates was analyzed by Western blot analyses.

sion during sake fermentation, K701 shows statistically significantly stronger expression of ribosome-associated genes with an RNA polymerase A and C (PAC) motif (under the control of Sfp1p) and weaker expression of GAAC genes with a Gcn4p-responsive element (GCRE) and stress response genes with an Msn2/4p-responsive element (STRE) than X2180 (3). Comparison of the gene expression profiles (see Fig. S1 in the supplemental material) indicated that the Sfp1p-dependent genes are rapidly downregulated, while GAAC and NCR genes are transiently upregulated early in sake fermentation in X2180. These results suggest that TORC1 activity is decreased after the onset of alcoholic fermentation using X2180. In contrast, these transcriptomic traits were less clearly observed in K701, implying a slower decline in TORC1 activity during the initial stage of alcoholic fermentation by K701.

To directly monitor TORC1 activity, an antibody against phospho-Thr737 of Sch9p (28) was used, as this TORC1-dependent phosphorylation of Sch9p is known to mediate signaling to Rim15p. Laboratory yeast and K701 lineage sake yeast cells engineered to overexpress 3HA-tagged Sch9p from a glycolytic gene promoter were sampled during alcoholic fermentation in YPD20 medium (1% yeast extract, 2% peptone, and 20% glucose). The sake strain exhibited a higher rate of carbon dioxide emission and completed alcoholic fermentation more rapidly than the laboratory strain (Fig. 2A). Phosphorylation of Sch9p Thr737 was detected only at the initial stage (at 6 h from the onset of alcoholic fermentation) and was more prominent in the sake strain than in the laboratory strain (Fig. 2B). The signals decayed quickly over time in both strains, suggesting that TORC1 activity is highest at the onset of alcoholic fermentation. It should be noted that the glycolytic promoter used in this study was inactivated after the completion of logarithmic phase (>12 to 24 h) and that 3HA-Sch9p was expressed at only low levels after 2 days. It is also worth noting that the abundance of 3HA-Sch9p may suggest that the glycolytic promoter activity remains longer in sake yeast cells than in laboratory yeast cells, which may be another plausible explanation of the high fermentation performance of sake yeast cells.

Effects of the TORC1-Greatwall-PP2A$^{B55\delta}$ pathway on fermentation performance. In *S. cerevisiae* laboratory strains, loss of Rim15p leads to an increase in the initial rate of carbon dioxide emission during alcoholic fermentation (5, 7) (Fig. 3A). To examine whether TORC1 acts as a negative regulator of Rim15p activity in fermentation control, we tested the effect of altered TORC1 signaling on fermentation performance in a laboratory strain (Fig. 3, red graphs). Addition of a low concentration (1 nM) of the TORC1 inhibitor rapamycin to the medium led to a decrease in the rate of carbon dioxide emission from day 1.5 to 4 (Fig. 3B). Since cell growth was not severely affected by 1 nM rapamycin (data not shown), the observed attenuation of carbon dioxide production was most likely indicative of reduced cellular fermentation performance.

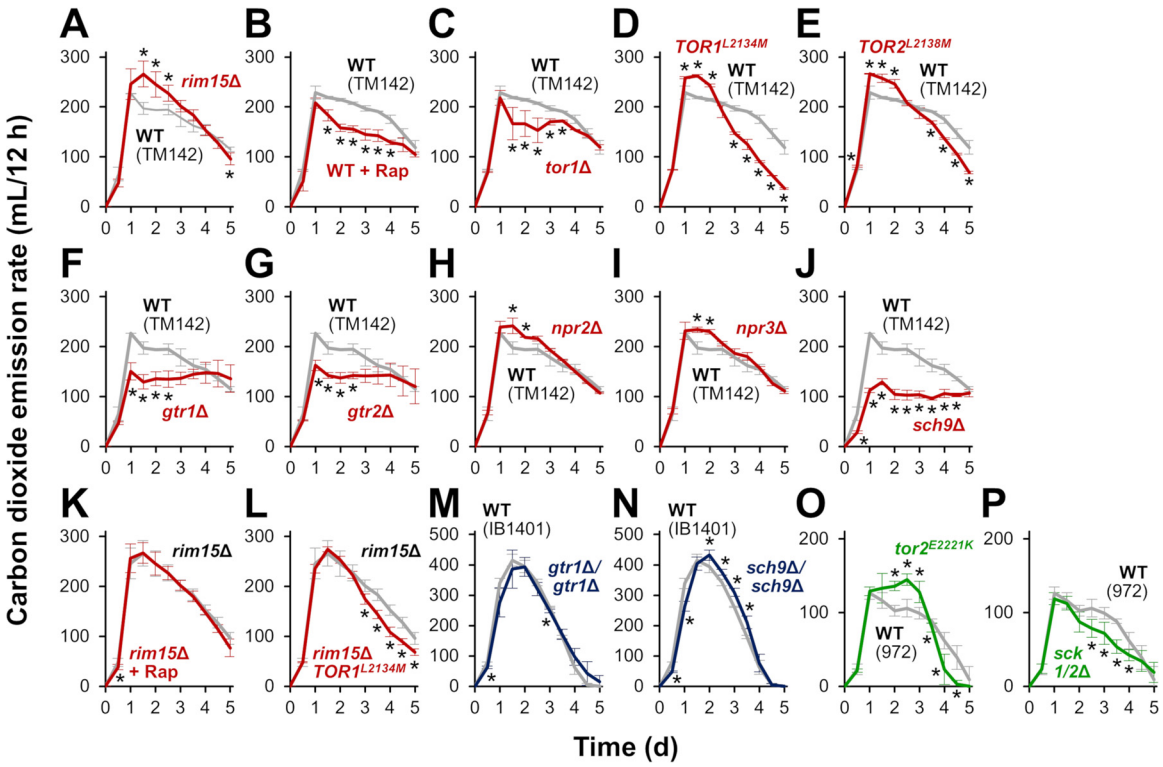

FIG 3 Effects of modification of the TORC1-Greatwall pathway on fermentation progression. Fermentation was monitored by measuring carbon dioxide emission. (A) Fermentation profiles of strain TM142 (wild type; gray) and its *rim15*Δ disruptant (red). (B) Fermentation profiles of strain TM142 in YPD20 medium in the absence (wild type; gray) or presence (red) of 1 nM rapamycin. (C to J) Fermentation profiles of strain TM142 (wild type; gray) and its *tor1*Δ (C), $TOR1^{L2134M}$ (D), $TOR2^{L2138M}$ (E), *gtr1*Δ (F), *gtr2*Δ (G), *npr2*Δ (H), *npr3*Δ (I), or *sch9*Δ (J) mutant (red). (K) Fermentation profiles of strain TM142 *rim15*Δ in YPD20 medium in the absence (gray) or presence (red) of 1 nM rapamycin. (L) Fermentation profiles of strain TM142 *rim15*Δ (gray) and its $TOR1^{L2134M}$ mutant (red). (M and N) Fermentation profiles of strain IB1401 (wild type; gray) and its *gtr1*Δ/*gtr1*Δ (M) or *sch9*Δ/*sch9*Δ (N) disruptant (blue). (O and P) Fermentation profiles of the wild-type *S. pombe* strain (gray) and its $tor2^{E2221K}$ (O) or *sck1/2*Δ (P) mutant (green). Fermentation tests were performed in YPD20 medium (A to N) or in YPD10 medium (O and P) at 30°C for 5 days. Values represent the mean ± SD of data from two or more independent experiments. *, significantly different from the value for the control experiment (*t* test, $P < 0.05$). Note that the data from experiments using laboratory, sake, and fission yeast strains are indicated in red, blue, and green, respectively. WT, wild type; Rap, rapamycin.

Deletion of the *TOR1* gene, which encodes a nonessential catalytic subunit of TORC1, also decreased carbon dioxide emission from day 1.5 to 3.5 (Fig. 3C). Deletion of *TOR2*, which encodes a second TOR kinase that can also serve as a catalytic subunit of TORC1, was not tested in this study because Tor2p is essential for cell viability in *S. cerevisiae*. In contrast, the hyperactive *TOR1* and *TOR2* alleles ($TOR1^{L2134M}$ and $TOR2^{L2138M}$) (28) increased carbon dioxide emission around day 1 to 2 (Fig. 3D and E). Strains harboring either of these hyperactive alleles exhibited drastic decreases in the rate of carbon dioxide emission toward the end of the fermentation tests. Excess TORC1 activity might prevent yeast cells from acquiring stress tolerance, leading to cell death caused by higher concentrations of ethanol on later days. These results suggested that TORC1 activity correlates with fermentation performance during the initial stage of the process. Indeed, deletion of *GTR1* or *GTR2*, activators of TORC1 signaling, decreased carbon dioxide emission (Fig. 3F and G). In addition, disruption of *NPR2* or *NPR3*, which encode the components of the SEACIT subcomplex that inhibit TORC1 signaling, resulted in increased carbon dioxide emission around day 1.5 to 2 (Fig. 3H and I), corroborating the role of TORC1 as a positive regulator of alcoholic fermentation. On the other hand, loss of Sch9p, which mediates signaling between TORC1 and Rim15p (Fig. 1), markedly decreased carbon dioxide emission (Fig. 3J).

Next, the effects of TORC1 on fermentation performance were examined in the Rim15p-deficient strains from both laboratory and sake yeast backgrounds. In *rim15*Δ cells of the laboratory strain, 1 nM rapamycin did not affect carbon dioxide emission

(Fig. 3K). We confirmed that the growth of *rim15*Δ cells was not affected by 1 nM rapamycin (data not shown). In the *rim15*Δ background, the hyperactive *TOR1*^{L2134M} allele did not increase the initial rate of carbon dioxide emission (1 to 2 days) but caused a decrease in the later stage of fermentation (>3 days) (Fig. 3L). These data suggested that Rim15p is required for the TORC1-triggered fermentation control, specifically in the early stage of alcoholic fermentation. Considering that the sake strains carry a homozygous loss-of-function mutation, *rim15*$^{5054\_5055insA}$ (5), it was predicted that the fermentation performance of the sake strain is not affected by TORC1 signaling. As expected, deletion of the *GTR1* or *SCH9* gene in the sake strain did not change the maximum rate of carbon dioxide emission (Fig. 3M and N, blue graphs), although alcoholic fermentation was slightly delayed in both cases, probably due to slower cell growth. Is the TORC1-dependent fermentation control evolutionarily conserved among different yeast species? To address this point, we also assessed whether the conserved TORC1 pathway affects fermentation performance in the fission yeast *S. pombe* (Fig. 3, green graphs). As observed in budding yeast, an activated allele of *tor2*$^{+}$ (encoding a catalytic subunit of TORC1 in *S. pombe*), *tor2*^{E2221K} (29), brought about increased carbon dioxide emission in fission yeast (Fig. 3O). Furthermore, deletion of the redundant Sch9p-orthologous genes, *sck1*$^{+}$ and *sck2*$^{+}$, resulted in decreased carbon dioxide emission (Fig. 3P).

Does Greatwall-triggered signaling to PP2A$^{B55\delta}$ play a role in the control of alcoholic fermentation? To address this, we tested the effect of the altered Greatwall-ENSA-PP2A$^{B55\delta}$ pathway on fermentation performance in a laboratory strain (Fig. 4, red graphs) and a sake strain (blue graphs) of *S. cerevisiae*, as well as in *S. pombe* (green graphs). Deletion of the redundant ENSA-encoding genes *IGO1* and *IGO2* (*IGO1/2*), which mediate the signaling between Greatwall and PP2A$^{B55\delta}$ in *S. cerevisiae* (Fig. 1), led to an increased rate of carbon dioxide emission, as did deletion of *RIM15* (Fig. 4A and B). Similarly, in *S. pombe*, both the *cek1*Δ *ppk18*Δ and *igo1*Δ strains, which lack Greatwall and ENSA, respectively (17), exhibited higher rates of carbon dioxide emission than did the wild type (Fig. 4C and D). PP2A is a heterotrimeric enzyme complex composed of structural (A), regulatory (B), and catalytic (C) subunits. In budding yeast, the loss of both C subunit-encoding genes *PPH21* and *PPH22* leads to cell death, but disruption of either gene alone only weakly decreased carbon dioxide emission (Fig. 4E and F). In addition, deletion of the A subunit-encoding *TPD3* gene inhibited alcoholic fermentation (Fig. 4G). Moreover, deletion of *CDC55*, which encodes a B55δ family regulatory subunit, severely decreased the rate of carbon dioxide emission throughout the duration of fermentation, whereas deletion of *RTS1*, which encodes a B56 family regulatory subunit, promoted alcoholic fermentation (Fig. 4H and I). In *S. pombe*, loss of the *ppa1*$^{+}$ or *ppa2*$^{+}$ gene, which encode C subunit isoforms, did not appear to affect alcoholic fermentation; however, loss of the *pab1*$^{+}$ gene, encoding a B55δ subunit, impaired alcoholic fermentation (Fig. 4J to L). Together, these data suggested that the Greatwall-ENSA-PP2A$^{B55\delta}$ pathway is involved in the control of alcoholic fermentation in both *S. cerevisiae* and *S. pombe*. When combined with the Greatwall or ENSA defects, deletion of the *CDC55* (*S. cerevisiae*) or *pab1*$^{+}$ (*S. pombe*) gene almost fully canceled high fermentation performance (Fig. 4M to O). Thus, PP2A$^{B55\delta}$ is likely the major target of Greatwall and ENSA in the control of alcoholic fermentation in both yeasts. Based on these data, it was hypothesized that PP2A$^{B55\delta}$ is responsible for the high fermentation performance of sake yeast strains.

Consistent with a previous report (5), expression of the functional *RIM15* gene derived from a laboratory strain did not attenuate alcoholic fermentation in the sake strain (Fig. 4P). Therefore, we next evaluated the role of PP2A$^{B55\delta}$ downstream of Rim15p in the high fermentation performance of sake yeast cells. Interestingly, we found that the diploid sake strain K701 is heterozygous for the deletion of a single adenine nucleotide at position 1092 of the *CDC55* gene (designated the *cdc55*^{MT} allele), resulting in a frameshift and premature polypeptide termination (Fig. 5A); thus, K701 carries only one functional *CDC55* allele (designated the *CDC55*^{WT} allele). To directly test the role of PP2A$^{B55\delta}$ in the sake yeast, the K701 strain was mutagenized by introduction

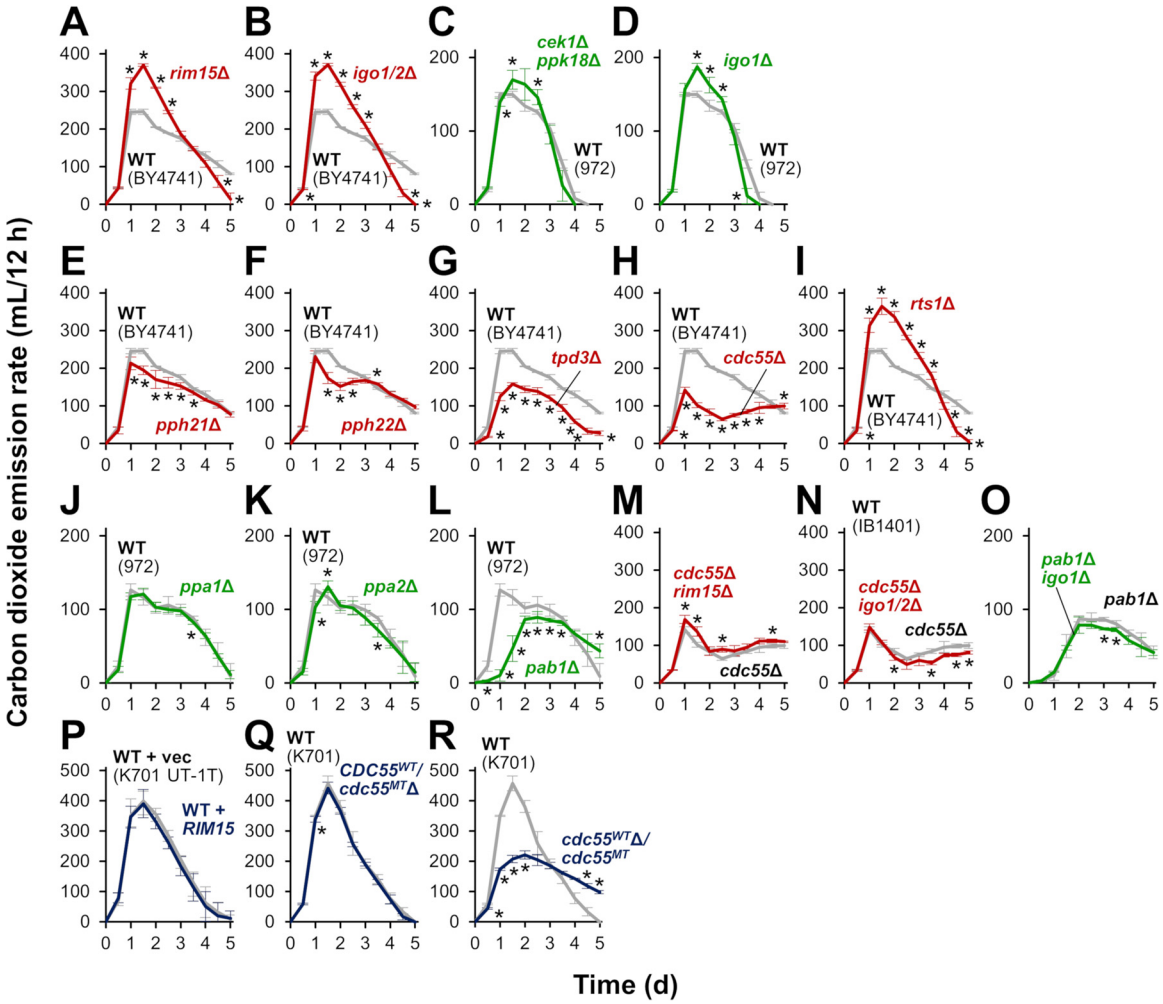

FIG 4 Effects of modification of the Greatwall-PP2A$^{B55\delta}$ pathway on fermentation progression. Fermentation was monitored by measuring carbon dioxide emission. (A and B) Fermentation profiles of strain BY4741 (wild type; gray) and its *rim15*Δ (A) or *igo1/2*Δ (B) disruptant (red). (C and D) Fermentation profiles of the wild-type *S. pombe* strain (gray) and its *cek1*Δ/*ppk18*Δ (C) or *igo1*Δ (D) disruptant (green). (E to I) Fermentation profiles of strain BY4741 (wild type; gray) and its *pph21*Δ (E), *pph22*Δ (F), *tpd3*Δ (G), *cdc55*Δ (H), or *rts1*Δ (I) disruptant (red). (J to L) Fermentation profiles of the wild-type *S. pombe* strain (gray) and its *ppa1*Δ (J), *ppa2*Δ (K), or *pab1*Δ (L) disruptant (green). (M and N) Fermentation profiles of strain BY4741 *cdc55*Δ (gray) and its *rim15*Δ (M) or *igo1/2*Δ (N) disruptant (red). (O) Fermentation profiles of the *S. pombe pab1*Δ strain (gray) and its *igo1*Δ disruptant (green). (P) Fermentation profiles of strain K701 UT-1T with an empty vector (wild type; gray) and with a functional *RIM15*-expressing plasmid (blue). (Q and R) Fermentation profiles of strain K701 (wild type; gray) and its *CDC55*^{WT}/*cdc55*^{MT}Δ (Q) or *cdc55*^{WT}Δ/*cdc55*^{MT} (N) disruptant (blue). Fermentation tests were performed in YPD20 medium (A, B, E to I, M, N, and P to R) or in YPD10 medium (C, D, J to L, and O) at 30°C for 5 days. Values represent the mean ± SD of data from two or more independent experiments. *, significantly different from the value for the control experiment (*t* test, $P < 0.05$). Note that the data from experiments using laboratory, sake, and fission yeast strains are indicated by red, blue, and green, respectively. WT, wild type.

of a *CDC55*-disrupting construct, yielding 12 heterozygous disruptants. Direct sequencing of the *CDC55* loci amplified from genomic DNA revealed that the *cdc55*^{MT} allele was disrupted in six of the heterozygous disruptants, while the *CDC55*^{WT} allele was disrupted in the other six heterozygous disruptants. The former class, in which the *CDC55*^{WT} allele remains intact, exhibited fermentation characteristics similar to those of the parental K701 strain (Fig. 4Q), while the latter class, with no functional *CDC55* gene, exhibited markedly lower carbon dioxide emission, especially in the initial stage of fermentation (0.5 to 2 days) (Fig. 4R). These results indicated that the *CDC55*^{WT} allele is required for the high fermentation performance of the K701 sake yeast strain.

Heterozygous nonsense or frameshift mutations in the *CDC55* gene of the sake yeast strains. As mentioned above, we identified a heterozygous loss-of-function mutation (*cdc55*^{1092delA}) in diploid K701 (Fig. 5A). To test whether this mutation is conserved among the sake strains, we analyzed the sequences of the *CDC55* genes in

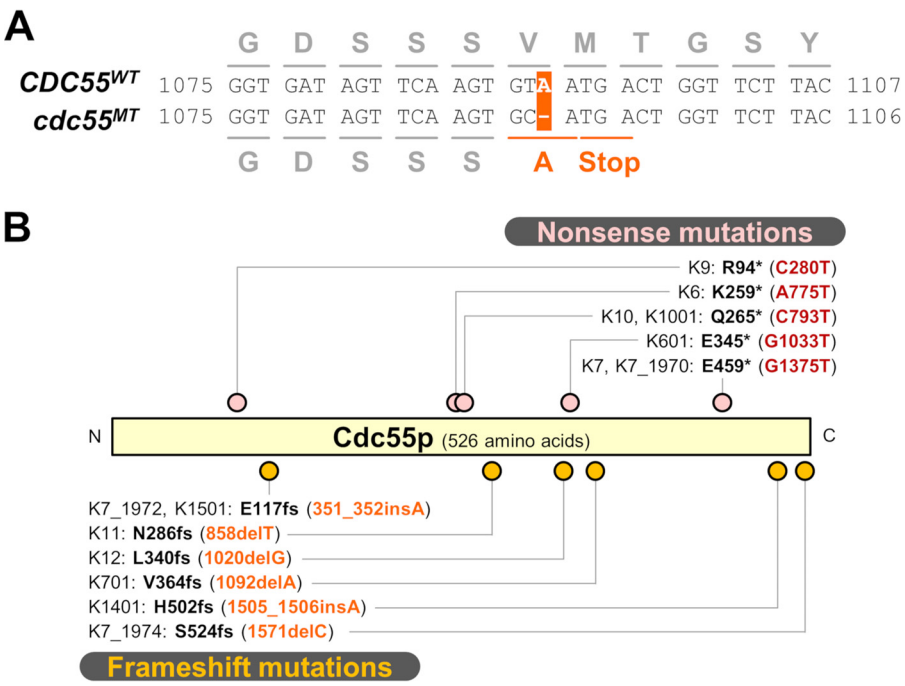

FIG 5 Heterozygous nonsense or frameshift mutations found in the *CDC55* genes of K7-related sake strains. (A) The *cdc55*^{1092delA} (also known as *cdc55*^{MT}) mutation unique to K701. In this loss-of-function allele of K701, deletion of a single adenine nucleotide at open reading frame (ORF) nucleotide 1092 causes a premature stop codon. (B) Mutation sites of the *CDC55* gene of K7-related sake strains. Nonsense and frameshift mutation sites are indicated by pink and orange dots, respectively. fs, frameshift.

17 K7-related Kyokai sake strains, i.e., K6, K601, K7, K701, K9, K901, K10, K1001, K11, K12, K13, K14, K1401, K1501, K1601, K1701, and K1801. (Note that the numbering corresponds to the sequential isolation of these strains. The "01" suffix is used to indicate foamless variants that do not generate thick foam layers during sake fermentation; for instance, K701 is the foamless variant of K7 [30].) As shown in Fig. 5B, the *cdc55*^{1092delA} mutation is unique to K701, and 65% (11 of 17) of the tested strains contain other nonsense or frameshift mutations in the open reading frame of the *CDC55* gene. Notably, the three most recently isolated strains, K1601, K1701, and K1801, have neither a nonsense mutation nor a frameshift mutation in this locus. Although there are a few lineage-specific mutations, such as *cdc55*^{C793T} in K10 and K1001 and *cdc55*$^{351\_352insA}$ in K7 and K1501 (2), closely associated strains do not always contain the same mutation (e.g., K6 versus K601, K7 versus K701, or K7 versus K11). Each year, every Kyokai sake yeast strain was selected from clone stocks before distribution by the Brewing Society of Japan; notably, the K7 strains from three different years (1970, 1972, and 1974) carry distinct *cdc55* mutations. The K7 strain used for whole-genome analysis (4) harbors a *cdc55* mutation identical to the *cdc55*^{1571delC} allele in K7_1970. Thus, it appears that most of the *cdc55* mutations represent independent events that occurred after the establishment of the individual sake strains. While the *cdc55*^{1571delC} mutation in K7_1974 results in an additional 27 amino acid residues at the carboxyl terminus of the encoded protein, each of the other frameshift mutations leads to a premature stop codon that truncates the carboxyl terminus. Since all of the identified mutations are heterozygous, the effects of the *cdc55* loss-of-function mutations may be masked by the functional *CDC55* allele, as observed in K701.

Effects of PP2A$^{B55\delta}$ on the intracellular levels of glycolytic intermediates. Since PP2A$^{B55\delta}$ dephosphorylates many cellular substrates (31), it is difficult to infer how PP2A$^{B55\delta}$ controls alcoholic fermentation. However, it may be worth examining whether PP2A$^{B55\delta}$ regulates the activities of carbon metabolic enzymes through protein dephosphorylation, as several recent studies have shed light on posttranslational

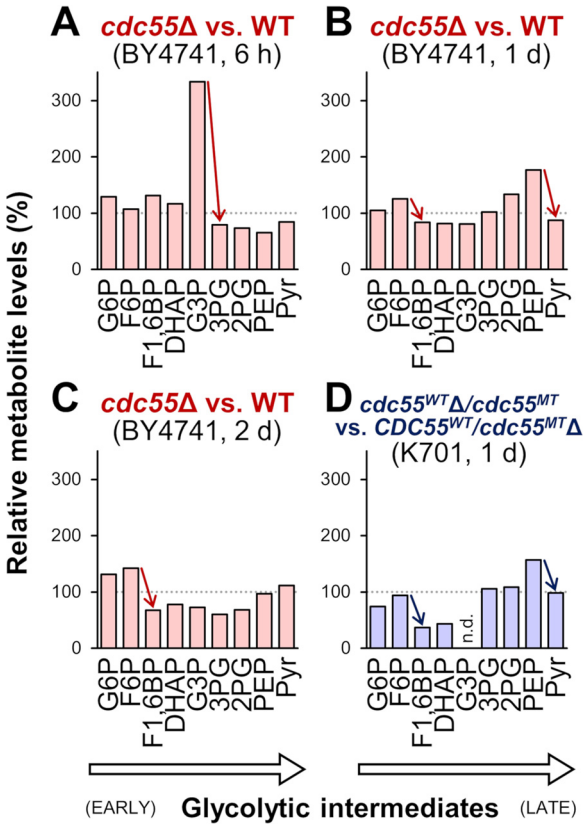

FIG 6 Effects of Cdc55p on glycolytic intermediate levels in the early stage of alcoholic fermentation. (A to C) Intracellular metabolite levels of laboratory strain BY4741 *cdc55*Δ at 6 h (A), 1 day (B), and 2 days (C) from the onset of alcoholic fermentation; values are normalized to those of the wild-type BY4741 at the respective time point. (D) Intracellular metabolite levels of sake strain K701 $cdc55^{WT}\Delta/cdc55^{MT}$ at 1 day from the onset of alcoholic fermentation; values are normalized to those of K701 $CDC55^{WT}/cdc55^{MT}\Delta$. Red and blue arrows indicate notable differences between adjacent metabolites. Each datum provided is from a single experiment from a representative fermentation test. G6P, glucose 6-phosphate; F6P, fructose 6-phosphate; F1,6BP, fructose 1,6-bisphosphate; DHAP, dihydroxyacetone phosphate; G3P, glyceraldehyde 3-phosphate; 3PG, 3-phosphoglyceric acid; 2PG, 2-phosphoglyceric acid; PEP, phosphoenolpyruvic acid; Pyr, pyruvic acid; n.d., not determined. Note that G3P was not detected in K701 $cdc55^{WT}\Delta/cdc55^{MT}$ and that 1,3-bisphosphoglyceric acid (1,3BPG) was not detected in any of the samples.

modifications as regulatory mechanisms for metabolic flux *in vivo* (32, 33). In the present study, we adopted a metabolomic approach to explore the glycolytic reactions that may be affected by the loss of $PP2A^{B55\delta}$ function. Metabolites were extracted from cells sampled at the early stages (6 h, 1 day, or 2 days) of alcoholic fermentation in YPD20 medium. Relative metabolite levels at 6 h indicated that the pools of early glycolytic intermediates (glucose 6-phosphate [G6P], fructose 6-phosphate [F6P], fructose 1,6-bisphosphte [F1,6BP], and dihydroxyacetone phosphate [DHAP]) were slightly increased by deletion of the *CDC55* gene in the laboratory strain BY4741 (Fig. 6A). In contrast, the level of glyceraldehyde 3-phosphate (G3P) accumulated in *cdc55*Δ cells was 3-fold higher than that in wild-type cells, while the intracellular pools of 3-phosphoglyceric acid (3PG) and the ensuing glycolytic intermediates were smaller in *cdc55*Δ cells. These data suggest that, at 6 h, the metabolic steps between G3P and 3PG are specifically compromised by deletion of the *CDC55* gene. We noted that 1,3-bisphosphoglyceric acid (1,3BPG), an intermediate between G3P and 3PG in the glycolytic pathway, was not detected in either wild-type or *cdc55*Δ cells in the present analysis. At 1 day, similar accumulations were observed for F6P and phosphoenolpyruvic acid (PEP) in *cdc55*Δ cells (Fig. 6B); the accumulation of F6P remained even at 2 days (Fig. 6C). These data suggested that, at 1 to 2 days, the metabolic steps between F6P and F1,6BP, and between PEP and pyruvic acid, are disturbed by deletion of the

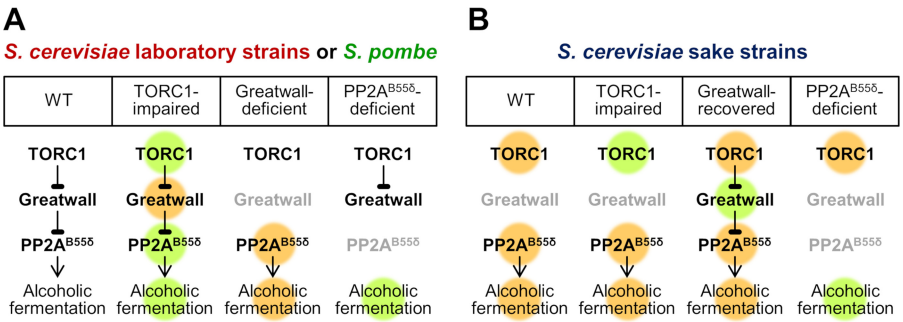

FIG 7 A hypothetical model of the regulation of fermentation control by the TORC1-Greatwall-PP2A$^{B55\delta}$ pathway. Orange and green indicate activities higher and lower, respectively, than those of *S. cerevisiae* wild-type laboratory strains. (A) In *S. cerevisiae* laboratory strains and *S. pombe*, changes in the activity of TORC1, Greatwall, or PP2A$^{B55\delta}$ may lead to altered alcoholic fermentation performance. (B) In *S. cerevisiae* sake strains, both the high TORC1 activity and the loss of Rim15p may contribute to the constitutively high PP2A$^{B55\delta}$ activity. Thus, PP2A$^{B55\delta}$ must be disrupted to impair the fermentation performance in these strains.

CDC55 gene. In the sake strain K701 at 1 day from the onset of alcoholic fermentation, the accumulations of F6P and PEP were observed in *CDC55*^{WT}-deficient cells (*cdc55*$^{WT}\Delta$/*cdc55*^{MT}) (Fig. 6D), consistent with the results obtained using laboratory yeast cells. Based on these results, it is possible to hypothesize that the enzymatic activity of phosphofructokinase (F6P to F1,6BP) is reproducibly negatively affected by the loss of PP2A$^{B55\delta}$ function in both laboratory and sake strains when the fermentation rates reach their maxima.

DISCUSSION

Although the genes and enzymes of the glycolysis and alcoholic fermentation pathways have been thoroughly studied in *S. cerevisiae*, the mechanisms by which intracellular signaling pathways regulate carbohydrate metabolism in response to extracellular cues are still not fully elucidated. We previously identified a loss-of-function mutation in the *RIM15* gene (*rim15*$^{5054\_5055insA}$) that is present in K7 and shared among the associated sake yeast strains, suggesting that this mutation is associated with enhanced fermentation performance (5, 7). In the present work, we showed that sake yeast cells exhibit elevated TORC1 activity during alcoholic fermentation in comparison to laboratory strains. TORC1 upregulates the Sfp1p-targeted genes encoding ribosome-associated proteins and downregulates members of the NCR and GAAC regulons in a Rim15p-independent manner (27). These attributes (see Fig. S1 in the supplemental material), as well as the observed defect in induction of the Msn2/4p-mediated stress-response genes (3), suggest enhanced activation of TORC1 in sake yeast cells (compared to laboratory strains). The high level of phosphorylated Thr737 of Sch9p observed in sake yeast cells (Fig. 2) is consistent with this idea. As previously reported, TORC1 activity is not fully attenuated in K7 cells even under nitrogen limitation (34). Therefore, elevated TORC1 activity can be regarded as a novel hallmark of the sake yeast cells. In general, nutritional limitation and environmental stresses rapidly inactivate TORC1 in yeast, resulting in inhibition of cell growth and proliferation. We postulate that the maintenance of high TORC1 activity in sake yeast cells may facilitate cellular metabolic activity even under fermentative conditions. Among the components of TORC1, only Tor1p contains missense mutations (R167Q and T1456I) in K7 and its relatives. Further studies will be needed to evaluate the roles of the mutations in *TOR1* and those in other genes to be discovered in sake yeast strains.

In the present study, we demonstrated that the conserved TORC1-Greatwall-PP2A$^{B55\delta}$ pathway is key to the control of alcoholic fermentation (Fig. 7A). In *S. cerevisiae* laboratory strains and *S. pombe*, altered TORC1 activities led to changes in fermentation performance, specifically at the early stage of alcoholic fermentation. However, in laboratory yeast cells deficient in Greatwall, the initial rate of alcoholic

fermentation was maintained and was not affected by changes in TORC1. It should be also noted that Greatwall does not affect the fermentation performance in a TORC1-hyperactivated strain (compare the fermentation profiles of *TOR1*^{L2134M} in Fig. 3D and *rim15*Δ *TOR1*^{L2134M} in Fig. 3L). In contrast, in PP2A$^{B55\delta}$-deficient laboratory yeast cells, the fermentation rate was strikingly low and was not enhanced even by a loss of Greatwall or ENSA. The observed strong epistasis suggested that the Greatwall-PP2A$^{B55\delta}$ pathway, among numerous downstream effector proteins of TORC1, is the primary mediator of fermentation control. This epistasis also indicated that PP2A$^{B55\delta}$ is the major regulator of the alcoholic fermentation machinery.

In our hypothesis, both high TORC1 activity and loss of Rim15p contribute to the activation of PP2A$^{B55\delta}$ and the subsequent enhancement of the cellular fermentation performance in the K7-related sake strains (Fig. 7B). Indeed, neither impairment of TORC1 nor recovery of Rim15p is sufficient to attenuate PP2A$^{B55\delta}$ activity in these cells. Presumably, even if TORC1 activity is decreased, the change in TORC1 signaling may not be conveyed downstream due to the loss of Rim15p (Fig. 1). On the other hand, if a functional *RIM15* gene is restored, the hyperactivated TORC1 can inhibit the functions of Rim15p, resulting in elevated PP2A$^{B55\delta}$ activity. Our data indicated that the high fermentation performance of sake yeast cells was abrogated only when the functional *CDC55* (B55δ-encoding) gene was disrupted (Fig. 4R). Consequently, the two changes (in TORC1 and Rim15p) observed in the TORC1-Greatwall-PP2A$^{B55\delta}$ pathway of sake yeast cells may mutually ensure the robust phenotype of these strains in the context of alcoholic fermentation.

Why do multiple sake yeast strains possess putative loss-of-function mutations (i.e., nonsense mutations and frameshift mutations [Fig. 5B]) in the *CDC55* gene? Since diploid sake yeast strains contain two copies of the *CDC55* gene, heterozygosity for a loss-of-function mutation at the loci may not yield apparent effects on alcoholic fermentation. In fact, the most recently isolated strains, K1601, K1701, and K1801, which do not contain any nonsense or frameshift mutations, exhibit high fermentation performance as the other sake strains do. PP2A$^{B55\delta}$ regulates not only carbohydrate metabolism but also cell cycle progression. In *S. cerevisiae*, PP2A$^{B55\delta}$ is the key inhibitor of the entry into quiescence (G_0 phase). Loss of Rim15p decreases the expression of stress response genes and shortens chronological life span, and *cdc55*Δ is able to suppress such Rim15p-deficient phenotypes (24). The heterozygous loss-of-function mutations in *CDC55* in the sake strains may reduce the dosage of functional Cdc55p, thereby serving as weak suppressors of the long-term survival defect associated with the *rim15*$^{5054\_5055insA}$ mutation (see Fig. S2 in the supplemental material). Thus, the individual sake strains may have independently acquired and maintained the heterozygous *cdc55* mutations during decades of adaptation. If another mutation in the functional *CDC55* allele or a loss-of-heterozygosity (LOH) event occurs, the lack of Cdc55p function further enhances cell viability but severely impairs fermentation performance. Based on our model, the heterozygous *cdc55* mutations may decrease the genetic stability for high fermentation performance and thus should be eliminated to facilitate the development of genetically stable sake yeast strains.

Comparison of the glycolytic intermediate pools between wild-type and *cdc55*Δ cells suggested that the loss of PP2A$^{B55\delta}$ negatively affects the metabolic reactions responsible for the conversion of (i) F6P to F1,6BP, (ii) G3P to 3PG, and (iii) PEP to pyruvic acid during the initial stage of alcoholic fermentation (Fig. 6). We presume that these defects are at least partially responsible for the low fermentation performance of *cdc55*Δ cells. Intriguingly, PP2A$^{B55\delta}$ appears to control individual glycolytic reactions in a fermentation phase-specific manner; only the defect in conversion of G3P to 3PG was observed at 6 h from the onset of alcoholic fermentation in a laboratory strain, whereas the defects in conversion of F6P to F1,6BP and/or of PEP to pyruvic acid were observed from 1 day to 2 days. Thus, these results imply that the activities of glycolytic enzymes are separately regulated during alcoholic fermentation and that the pleiotropic functions of PP2A$^{B55\delta}$ contribute to the optimal glycolytic flux. Among the glycolytic enzymes, phosphofructokinase and pyruvate kinase catalyze irreversible and rate-

limiting reactions, i.e., conversion of F6P to F1,6BP and of PEP to pyruvic acid, respectively, in glycolysis. Recent integrated phosphoproteomics data for budding yeast indicate that Pfk1p and Pfk2p (the α and β subunits of phosphofructokinase, respectively) and Cdc19p (the main pyruvate kinase isozyme) form phosphorylation hubs, suggesting that multiple protein kinases phosphorylate these enzymes to modulate their activity, intracellular localization, or protein degradation (32, 33). For example, it has been reported that phosphorylation of residue Ser163 of Pfk2p inhibits the phosphofructokinase activity *in vivo* under gluconeogenic conditions (35). The protein phosphatase activity of PP2A$^{B55\delta}$ may directly regulate glycolytic enzymes by counteracting such inhibitory phosphorylation. In fact, Pfk1p and Pfk2p are listed as putative PP2A$^{B55\delta}$-dephosphorylated proteins (31). The 3PG kinase Pgk1p, which is involved in the conversion of G3P to 3PG, also is a putative PP2A$^{B55\delta}$ target. The phosphorylation status and the activities of the candidate enzymes should be compared between wild-type and *cdc55*Δ cells during alcoholic fermentation. Since the glycolytic pathway and the posttranslational modifications of the glycolytic enzymes are often conserved evolutionarily, our study may also offer clues to identify novel key mechanisms of protein phosphorylation-mediated glycolytic control by the TORC1-Greatwall-PP2A$^{B55\delta}$ pathway.

MATERIALS AND METHODS

Yeast strains. The yeast strains used in this study are listed in Table 1. *Saccharomyces cerevisiae* laboratory strain BY4741 and its single-deletion mutants were obtained from the European *Saccharomyces cerevisiae* Archive for Functional Analysis (Euroscarf), Germany. Another *S. cerevisiae* laboratory strain, X2180, and *Schizosaccharomyces pombe* wild-type strain 972 were obtained from the American Type Culture Collection (ATCC), USA. Sake yeast strains Kyokai no. 7 (K7) and its relatives (K6, K601, K701, K9, K901, K10, K1001, K11, K12, K13, K14, K1401, K1501, K1601, K1701, and K1801) were provided by the Brewing Society of Japan (BSJ). *S. pombe* strain ED666 *cek1*Δ::*kanMX* (*h*$^+$ *ade6-M210 ura4-D18 leu1-32 cek1*Δ::*kanMX*) was obtained from Bioneer (Korea).

Disruption of the *IGO2* gene in BY4741 *igo1*Δ was performed using a PCR-based method (36) with the gene-specific primer pair IGO2-DF (5′-CAT ATA AAC AAA AAT ACG TAC CAA AGA AGT GTT ATA AAA GTG ATA TAA CTC GGA TCC CCG GGT TAA TTA A-3′) and IGO-DR (5′-TAG TGA TGA TAA AAA AAA AGT AAT ACC ACA TAA TAT CAT TCC TTC ATT AGG AAT TCG AGC TCG TTT AAA C-3′) and plasmid pFA6a-hphNT (37) as the template to generate BY4741 *igo1*Δ::*kanMX igo2*Δ::*hphNT* (BY4741 *igo1/2*Δ). Disruption of the *CDC55* gene in wild-type BY4741, BY4741 *rim15*Δ, and BY4741 *igo1/2*Δ was performed using a PCR-based method (36) with the gene-specific primer pair CDC55-DF (5′-AGG TCA AAC TGG AGA GAT CTT ACG CAT AAA GAA ATA TAA TAT AGC GCA CAC GGA TCC CCG GGT TAA TTA A-3′) and CDC55-DR (5′-GGG AAG ATA TGG GAT AAA AAA AAG TAA GGG AAA ATA AGG AAT TAT TAT AAG AAT TCG AGC TCG TTT AAA C-3′) and plasmid pFA6a-natNT (37) as the template to generate BY4741 *cdc55*Δ::*natNT* (BY4741 *cdc55*Δ), BY4741 *cdc55*Δ::*natNT rim15*Δ::*kanMX* (BY4741 *cdc55*Δ *rim15*Δ), and BY4741 *cdc55*Δ::*natNT igo1*Δ::*kanMX igo2*Δ::*hphNT* (BY4741 *cdc55*Δ *igo1/2*Δ), respectively.

The *TOR1*^{L2134M} mutation was previously reported as a hyperactive point mutation in the kinase domain of Tor1p (28). Since the mutation site was conserved in the *TOR2* gene, the corresponding mutation was also introduced to generate *TOR2*^{L2138M}. Disruption of the *RIM15* gene in wild-type TM142 or in TM142 *TOR1*^{L2134M} was performed using a PCR-based method (36) with the gene-specific primer pair RIM15-DF (5′-TTT CTC TTG CCT CAT TTG ATA GAA TAG ATA AGC CCA GTA GAG GAA GAC AGC GGA TCC CCG GGT TAA TTA A-3′) and RIM15-DR (5′-CAA AGT TTT TAT TCA GTT ATT TTT TTT AAT TAT CTT TAT CTT AAA ATT TAG AAT TCG AGC TCG TTT AAA C-3′) and plasmid pFA6a-kanMX (37) as the template to generate TM142 *rim15*Δ::*kanMX* (TM142 *rim15*Δ) and TM142 *TOR1*^{L2134M} *rim15*Δ::*kanMX* (TM142 *TOR1*^{L2134M} *rim15*Δ), respectively. TM142 *gtr1*Δ::*kanMX* (TM142 *gtr1*Δ; TS084), TM142 *gtr2*Δ::*kanMX* (TM142 *gtr2*Δ; TS087), and TM142 *sch9*Δ::*kanMX* (TM142 *sch9*Δ; TS858) were from the laboratory stock (28, 38).

Heterozygous disruption of the *CDC55* gene in K701 was performed using a PCR-based method (36) with the gene-specific primer pair CDC55-DF and CDC55-DR and plasmid pFA6a-natNT (37) as the template. Correct disruption of the *CDC55*^{WT} or *cdc55*^{MT} allele was confirmed by genomic PCR and direct DNA sequencing of the PCR product. Homozygous disruption of the *SCH9* gene in IB1401 was performed according to a previous report (34). To overexpress 3HA-tagged Sch9p from a glycolytic gene promoter in IB1401, plasmid p416-3HA-SCH9 (kindly gifted from Kevin Morano from the University of Texas, USA) was introduced into IB1401.

Disruption of the *ppk18*$^+$ and *igo1*$^+$ genes in wild-type strain 972 was performed using a PCR-based method (36) with a gene-specific primer pair and plasmid pFA6a-kanMX (37) as the template to generate 972 *ppk18*Δ::*kanMX* and 972 *igo1*Δ::*kanMX* (972 *igo1*Δ), respectively. The *kanMX* genes in ED666 *cek1*Δ::*kanMX* and 972 *ppk18*Δ::*kanMX* were replaced with *natMX* and *hphMX*, respectively, using a one-step marker switch (39) to generate ED666 *cek1*Δ::*natMX* and 972 *ppk18*Δ::*hphMX*, respectively. Both strains were mated and sporulated to generate the prototrophic double mutant 972 *cek1*Δ::*natMX ppk18*Δ::*hphMX* (972 *cek1*Δ *ppk18*Δ). To construct the prototrophic mutants 972 *sck1*Δ::*his7*$^+$ *sck2*Δ::*ura4*$^+$ (972 *sck1*Δ *sck2*Δ), 972 *ppa1*Δ::*ura4*$^+$ (*ppa1*Δ), *ppa2*Δ::*ura4*$^+$ (972 *ppa2*Δ), and 972 *pab1*Δ::*ura4*$^+$ (972 *pab1*Δ),

TABLE 1 Yeast strains used in this study

Species and strain	Genotype	Source or reference[a]
S. cerevisiae		
Laboratory strains		
BY4741 background with *RIM15*^{WT} and *CDC55*^{WT}		
BY4741	*MAT***a** *leu2Δ0 his3Δ1 ura3Δ0 met15Δ0*	Euroscarf
BY4741 *rim15Δ*	BY4741 *rim15Δ::kanMX*	Euroscarf
BY4741 *igo1Δ*	BY4741 *igo1Δ::kanMX*	Euroscarf
BY4741 *igo1/2Δ*	BY4741 *igo1Δ::kanMX igo2Δ::hphNT*	This study
BY4741 *pph21Δ*	BY4741 *pph21Δ::kanMX*	Euroscarf
BY4741 *pph22Δ*	BY4741 *pph22Δ::kanMX*	Euroscarf
BY4741 *tpd3Δ*	BY4741 *tpd3Δ::kanMX*	Euroscarf
BY4741 *cdc55Δ*	BY4741 *cdc55Δ::natNT*	This study
BY4741 *rts1Δ*	BY4741 *rts1Δ::kanMX*	Euroscarf
BY4741 *cdc55Δ rim15Δ*	BY4741 *cdc55Δ::natNT rim15Δ::kanMX*	This study
BY4741 *cdc55Δ igo1/2Δ*	BY4741 *cdc55Δ::natNT igo1Δ::kanMX igo2Δ::hphNT*	This study
X2180	*MAT***a**/α, wild type	ATCC
TM142 background with *RIM15*^{WT} and *CDC55*^{WT}		
TM142	*MATα leu2Δ1 his3Δ200 trp1Δ63 ura3-52*	28
TM142 *rim15Δ*	TM142 *rim15Δ::kanMX*	This study
TM142 *tor1Δ* (MY007)	TM142 *tor1Δ::kanMX*	This study
TM142 *TOR1*^{L2134M} (MY010)	TM142 *TOR1*^{L2134M}	This study
TM142 *TOR1*^{L2134M} *rim15Δ*	TM142 *TOR1*^{L2134M} *rim15Δ::kanMX*	This study
TM142 *TOR2*^{L2138M} (MY013)	TM142 *TOR2*^{L2138M}	This study
TM142 *gtr1Δ* (TS084)	TM142 *gtr1Δ::kanMX*	This study
TM142 *gtr2Δ* (TS087)	TM142 *gtr2Δ::kanMX*	This study
TM142 *npr2Δ* (TS232)	TM142 *npr2Δ::kanMX*	38
TM142 *npr3Δ* (TS236)	TM142 *npr3Δ::kanMX*	38
TM142 *sch9Δ* (TS858)	TM142 *sch9Δ::kanMX*	This study
TM142 P_{GPD}*-3HA-SCH9* (TS171)	TM142 *(natNT)*P_{GPD}*-3HA-SCH9*	28
Sake strains		
K701 background with *rim15*$^{5054\_5055insA}$/*rim15*$^{5054\_5055insA}$ and *CDC55*^{WT}/*cdc55*^{1092delA}		
K701	*MAT***a**/α, wild type; foamless variant of K7	BSJ
K701 *CDC55*^{WT}/*cdc55*^{MT}*Δ*	K701 *CDC55*^{WT}/*cdc55*^{MT}*Δ::natNT*	This study
K701 *cdc55*^{WT}*Δ/cdc55*^{MT}	K701 *cdc55*^{WT}*Δ::natNT/cdc55*^{MT}	This study
UT-1T	K701 *TRP1/trp1 ura3/ura3*	46
UT-1T + vector	K701 UT-1T(pAUR112)	5
UT-1T + *RIM15*	K701 UT-1T(pAUR112-ScRIM15)	5
IB1401	K701 *leu2Δ::loxP/leu2Δ::loxP his3Δ::loxP/his3Δ::loxP trp1/trp1 ura3/ura3*	47
K701 *gtr1Δ/gtr1Δ* (IB1663)	K701 *leu2Δ::loxP/leu2Δ::loxP trp1/trp1 ura3/ura3 gtr1Δ::CgLEU2/gtr1Δ::CgTRP1*	34
IB1401 *sch9Δ/sch9Δ* (IB1536)	IB1401 *sch9Δ::CgHIS3/sch9Δ::CgTRP1*	This study
IB1401 P_{GPD}*-3HA-SCH9* (IB1680)	IB1401(p416-3HA-SCH9)	This study
Other backgrounds with *rim15*$^{5054\_5055insA}$/*rim15*$^{5054\_5055insA}$		
K6		BSJ
K601	Foamless variant of K6	BSJ
K7		BSJ
K9		BSJ
K901	Foamless variant of K9	BSJ
K10		BSJ
K1001	Foamless variant of K10	BSJ
K11		BSJ
K12		BSJ
K13		BSJ
K14		BSJ
K1401	Foamless variant of K14	BSJ
K1501		BSJ
K1601		BSJ
K1701		BSJ
K1801		BSJ
S. pombe		
972	*h*$^{-}$, wild-type	ATCC
972 *tor2*^{E2221K} (CA8829)	*h*$^{-}$ *tor2*^{E2221K}*(kanMX)*	48
972 *sck1/2Δ* (CA7568)	*h*$^{-}$ *his7-366 ura4Δ18 sck1Δ::his7*$^{+}$ *sck2Δ::ura4*$^{+}$	This study
972 *cek1Δ ppk18Δ*	*h*$^{-}$ *cek1Δ::natMX ppk18Δ::hphMX*	This study
972 *igo1Δ*	*h*$^{-}$ *igo1Δ::kanMX*	This study
972 *ppa1Δ* (CA13052, CA13053)	*h*$^{-}$ *ura4-D18 ppa1Δ::ura4*$^{+}$	This study
972 *ppa2Δ* (CA13054, CA13055)	*h*$^{-}$ *ura4-D18 ppa2Δ::ura4*$^{+}$	This study
972 *pab1Δ* (CA13214, CA13215)	*h*$^{-}$ *ura4-D18 pab1Δ::ura4*$^{+}$	This study
972 *pab1Δ igo1Δ* (HT741)	*h*$^{-}$ *ura4-D18 pab1Δ::ura4*$^{+}$ *igo1Δ::kanMX*	This study

[a]Euroscarf, European *Saccharomyces cerevisiae* Archive for Functional Analysis (Germany); ATCC, American Type Culture Collection (United States); BSJ, Brewing Society of Japan (Japan).

a suitable wild-type strain was mated with JX766 (40), MY1121, MY1122 (41), and MY7214 (42), respectively, and sporulated. The *pab1*Δ and *igo1*Δ strains were mated and sporulated to generate the prototrophic double mutant 972 *pab1*Δ::*ura4*$^+$ *igo1*Δ::*kanMX* (972 *pab1*Δ *igo1*Δ).

Yeast cells were routinely grown in liquid YPD medium (1% yeast extract, 2% peptone, and 2% glucose) at 30°C, unless stated otherwise.

Sequencing of the *CDC55* gene. To analyze the *CDC55* sequence, the gene was amplified by PCR with the primer pair CDC55-(-150)-F (5′-GGC AGC TTA ATA CGA TTA CCC C-3′) and CDC55-(+1906)-R (5′-TGG TGA AGT GAT GAA AGA AGT CC-3′), using genomic DNA from the strain of interest as the template. The PCR product was sequenced directly using a BigDye Terminator v3.1 cycle sequencing kit (Thermo Fisher Scientific) and primers CDC55-seq2 (5′-TCG AGG TCA AAC TGG AGA GA-3′), CDC55-seq3 (5′-AAA ATC ATT GCT GCC ACC CC-3′), and CDC55-seq4 (5′-TGA TAC CTA TGA AAA CGA TGC GA-3′) on a 3130xl Genetic Analyzer (Applied Biosystems); sequencing was performed at Fasmac Co., Ltd. (Japan).

Fermentation tests. For measurements of fermentation rates, yeast cells were precultured in YPD medium at 30°C overnight, inoculated into 50 ml of YPD20 medium (1% yeast extract, 2% peptone, and 20% glucose) for *S. cerevisiae* or YPD10 medium (1% yeast extract, 2% peptone, and 10% glucose) for *S. pombe* at a final optical density at a wavelength of 600 nm (OD_{600}) of 0.1, and then further incubated at 30°C without shaking. Fermentation progression was continuously monitored by measuring the volume of evolved carbon dioxide gas using a Fermograph II apparatus (Atto) (43).

Analysis of intracellular metabolite profiles. During the fermentation tests in YPD20 medium, yeast cells corresponding to an OD_{600} of 20 were collected at 6 h, 1 day, or 2 days from the onset of the fermentation tests. All pretreatment procedures for the samples were performed according to the protocols provided by Human Metabolic Technologies, Inc. Briefly, each sample of yeast cells was washed twice with 1 ml ice-cold Milli-Q water, suspended in 1.6 ml methanol containing 5 μM internal standard solution 1 (Human Metabolic Technologies), and then sonicated for 30 s at room temperature. Cationic compounds were measured in the positive mode of capillary electrophoresis-time of flight mass spectrometry (CE-TOFMS), and anionic compounds were measured in the positive and negative modes of capillary electrophoresis-tandem mass spectrometry (CE-MS/MS) (44). Peaks detected by CE-TOFMS and CE-MS/MS were extracted using automatic integration software (MasterHands [Keio University] [45] and MassHunter Quantitative Analysis B.06.00 [Agilent Technologies], respectively) to obtain peak information, including *m/z*, migration time, and peak area. The peaks were annotated with putative metabolites from the HMT metabolite database (Human Metabolic Technologies) based on their migration times in CE and *m/z* values as determined by TOFMS and MS/MS. Metabolite concentrations were calculated by normalizing the peak area of each metabolite with respect to the area of the internal standard and by using standard curves, which were obtained from three-point calibrations.

SUPPLEMENTAL MATERIAL

Supplemental material for this article may be found at https://doi.org/10.1128/AEM.02083-18.

SUPPLEMENTAL FILE 1, PDF file, 0.1 MB.

ACKNOWLEDGMENTS

The Japan Society for the Promotion of Science (JSPS) provided funding to D.W. under grant number 16K18676, to S.I. under grant number 17H03795, and to T.M. under grant numbers 25291042 and 17H03802. The Public Foundation of Elizabeth Arnold-Fuji provided funding to D.W. The Foundation for the Nara Institute of Science and Technology provided funding to D.W. The Project of the NARO Bio-oriented Technology Research Advancement Institution (Research Program on Development of Innovative Technology) provided funding to H.T. under grant number 30017B.

We declare no conflicts of interest.

REFERENCES

1. Kitagaki H, Kitamoto K. 2013. Breeding research on sake yeasts in Japan: history, recent technological advances, and future perspectives. Annu Rev Food Sci Technol 4:215–235. https://doi.org/10.1146/annurev-food-030212-182545.
2. Ohnuki S, Okada H, Friedrich A, Kanno Y, Goshima T, Hasuda H, Inahashi M, Okazaki N, Tamura H, Nakamura R, Hirata D, Fukuda H, Shimoi H, Kitamoto K, Watanabe D, Schacherer J, Akao T, Ohya Y. 2017. Phenotypic diagnosis of lineage and differentiation during sake yeast breeding. G3 (Bethesda) 7:2807–2820. https://doi.org/10.1534/g3.117.044099.
3. Watanabe D, Wu H, Noguchi C, Zhou Y, Akao T, Shimoi H. 2011. Enhancement of the initial rate of ethanol fermentation due to dysfunction of yeast stress response components Msn2p and/or Msn4p. Appl Environ Microbiol 77:934–941. https://doi.org/10.1128/AEM.01869-10.
4. Akao T, Yashiro I, Hosoyama A, Kitagaki H, Horikawa H, Watanabe D, Akada R, Ando Y, Harashima S, Inoue T, Inoue Y, Kajiwara S, Kitamoto K, Kitamoto N, Kobayashi O, Kuhara S, Masubuchi T, Mizoguchi H, Nakao Y, Nakazato A, Namise M, Oba T, Ogata T, Ohta A, Sato M, Shibasaki S, Takatsume Y, Tanimoto S, Tsuboi H, Nishimura A, Yoda K, Ishikawa T, Iwashita K, Fujita N, Shimoi H. 2011. Whole-genome sequencing of sake yeast *Saccharomyces cerevisiae* Kyokai no. 7. DNA Res 18:423–434. https://doi.org/10.1093/dnares/dsr029.
5. Watanabe D, Araki Y, Zhou Y, Maeya N, Akao T, Shimoi H. 2012. A loss-of-function mutation in the PAS kinase Rim15p is related to defective quiescence entry and high fermentation rates of *Saccharomyces cerevisiae* sake yeast strains. Appl Environ Microbiol 78:4008–4016. https://doi.org/10.1128/AEM.00165-12.
6. Inai T, Watanabe D, Zhou Y, Fukada R, Akao T, Shima J, Takagi H, Shimoi H. 2013. Rim15p-mediated regulation of sucrose utilization during molasses fermentation using *Saccharomyces cerevisiae* strain PE-2. J Biosci Bioeng 116:591–594. https://doi.org/10.1016/j.jbiosc.2013.05.015.

7. Watanabe D, Zhou Y, Hirata A, Sugimoto Y, Takagi K, Akao T, Ohya Y, Takagi H, Shimoi H. 2016. Inhibitory role of Greatwall-like protein kinase Rim15p in alcoholic fermentation via upregulating the UDP-glucose synthesis pathway in *Saccharomyces cerevisiae*. Appl Environ Microbiol 82:340–351. https://doi.org/10.1128/AEM.02977-15.
8. Oomuro M, Kato T, Zhou Y, Watanabe D, Motoyama Y, Yamagishi H, Akao T, Aizawa M. 2016. Defective quiescence entry promotes the fermentation performance of bottom-fermenting brewer's yeast. J Biosci Bioeng 122:577–582. https://doi.org/10.1016/j.jbiosc.2016.04.007.
9. Watanabe D, Kaneko A, Sugimoto Y, Ohnuki S, Takagi H, Ohya Y. 2017. Promoter engineering of the *Saccharomyces cerevisiae RIM15* gene for improvement of alcoholic fermentation rates under stress conditions. J Biosci Bioeng 123:183–189. https://doi.org/10.1016/j.jbiosc.2016.08.004.
10. Pedruzzi I, Dubouloz F, Cameroni E, Wanke V, Roosen J, Winderickx J, De Virgilio C. 2003. TOR and PKA signaling pathways converge on the protein kinase Rim15 to control entry into G_0. Mol Cell 12:1607–1613. https://doi.org/10.1016/S1097-2765(03)00485-4.
11. Wanke V, Pedruzzi I, Cameroni E, Dubouloz F, De Virgilio C. 2005. Regulation of G_0 entry by the Pho80-Pho85 cyclin-CDK complex. EMBO J 24:4271–4278. https://doi.org/10.1038/sj.emboj.7600889.
12. Panchaud N, Péli-Gulli MP, De Virgilio C. 2013. Amino acid deprivation inhibits TORC1 through a GTPase-activating protein complex for the Rag family GTPase Gtr1. Sci Signal 6:ra42. https://doi.org/10.1126/scisignal.2004112.
13. Nicastro R, Sardu A, Panchaud N, De Virgilio C. 2017. The architecture of the Rag GTPase signaling network. Biomolecules 7:48. https://doi.org/10.3390/biom7030048.
14. Tatebe H, Shiozaki K. 2017. Evolutionary conservation of the components in the TOR signaling pathways. Biomolecules 7:77. https://doi.org/10.3390/biom7040077.
15. Urban J, Soulard A, Huber A, Lippman S, Mukhopadhyay D, Deloche O, Wanke V, Anrather D, Ammerer G, Riezman H, Broach JR, De Virgilio C, Hall MN, Loewith R. 2007. Sch9 is a major target of TORC1 in *Saccharomyces cerevisiae*. Mol Cell 26:663–674. https://doi.org/10.1016/j.molcel.2007.04.020.
16. Wanke V, Cameroni E, Uotila A, Piccolis M, Urban J, Loewith R, De Virgilio C. 2008. Caffeine extends yeast lifespan by targeting TORC1. Mol Microbiol 69:277–285. https://doi.org/10.1111/j.1365-2958.2008.06292.x.
17. Chica N, Rozalén AE, Pérez-Hidalgo L, Rubio A, Novak B, Moreno S. 2016. Nutritional control of cell size by the Greatwall-endosulfine-PP2A·B55 pathway. Curr Biol 26:319–330. https://doi.org/10.1016/j.cub.2015.12.035.
18. Düvel K, Yecies JL, Menon S, Raman P, Lipovsky AI, Souza AL, Triantafellow E, Ma Q, Gorski R, Cleaver S, Vander Heiden MG, MacKeigan JP, Finan PM, Clish CB, Murphy LO, Manning BD. 2010. Activation of a metabolic gene regulatory network downstream of mTOR complex 1. Mol Cell 39:171–183. https://doi.org/10.1016/j.molcel.2010.06.022.
19. Cameroni E, Hulo N, Roosen J, Winderickx J, De Virgilio C. 2004. The novel yeast PAS kinase Rim15 orchestrates G_0-associated antioxidant defense mechanisms. Cell Cycle 3:462–468.
20. Lee P, Kim MS, Paik SM, Choi SH, Cho BR, Hahn JS. 2013. Rim15-dependent activation of Hsf1 and Msn2/4 transcription factors by direct phosphorylation in *Saccharomyces cerevisiae*. FEBS Lett 587:3648–3655. https://doi.org/10.1016/j.febslet.2013.10.004.
21. Yu J, Fleming SL, Williams B, Williams EV, Li Z, Somma P, Rieder CL, Goldberg ML. 2004. Greatwall kinase: a nuclear protein required for proper chromosome condensation and mitotic progression in *Drosophila*. J Cell Biol 164:487–492. https://doi.org/10.1083/jcb.200310059.
22. Mochida S, Maslen SL, Skehel M, Hunt T. 2010. Greatwall phosphorylates an inhibitor of protein phosphatase 2A that is essential for mitosis. Science 330:1670–1673. https://doi.org/10.1126/science.1195689.
23. Gharbi-Ayachi A, Labbé JC, Burgess A, Vigneron S, Strub JM, Brioudes E, Van-Dorsselaer A, Castro A, Lorca T. 2010. The substrate of Greatwall kinase, Arpp19, controls mitosis by inhibiting protein phosphatase 2A. Science 330:1673–1677. https://doi.org/10.1126/science.1197048.
24. Bontron S, Jaquenoud M, Vaga S, Talarek N, Bodenmiller B, Aebersold R, De Virgilio C. 2013. Yeast endosulfines control entry into quiescence and chronological life span by inhibiting protein phosphatase 2A. Cell Rep 3:16–22. https://doi.org/10.1016/j.celrep.2012.11.025.
25. Moreno-Torres M, Jaquenoud M, De Virgilio C. 2015. TORC1 controls G_1-S cell cycle transition in yeast via Mpk1 and the greatwall kinase pathway. Nat Commun 6:8256. https://doi.org/10.1038/ncomms9256.
26. Moreno-Torres M, Jaquenoud M, Péli-Gulli MP, Nicastro R, De Virgilio C. 2017. TORC1 coordinates the conversion of Sic1 from a target to an inhibitor of cyclin-CDK-Cks1. Cell Discov 3:17012. https://doi.org/10.1038/celldisc.2017.12.
27. Conrad M, Schothorst J, Kankipati HN, Van Zeebroeck G, Rubio-Texeira M, Thevelein JM. 2014. Nutrient sensing and signaling in the yeast *Saccharomyces cerevisiae*. FEMS Microbiol Rev 38:254–299. https://doi.org/10.1111/1574-6976.12065.
28. Takahara T, Maeda T. 2012. Transient sequestration of TORC1 into stress granules during heat stress. Mol Cell 47:242–252. https://doi.org/10.1016/j.molcel.2012.05.019.
29. Urano J, Sato T, Matsuo T, Otsubo Y, Yamamoto M, Tamanoi F. 2007. Point mutations in TOR confer Rheb-independent growth in fission yeast and nutrient-independent mammalian TOR signaling in mammalian cells. Proc Natl Acad Sci U S A 104:3514–3519. https://doi.org/10.1073/pnas.0608510104.
30. Ouchi K, Akiyama H. 1971. Non-foaming mutants of sake yeasts selection by cell agglutination method and by froth flotation method. Agric Biol Chem 35:1024–1032. https://doi.org/10.1080/00021369.1971.10860043.
31. Baro B, Játiva S, Calabria I, Vinaixa J, Bech-Serra JJ, de LaTorre C, Rodrigues J, Hernáez ML, Gil C, Barceló-Batllori S, Larsen MR, Queralt E. 2018. SILAC-based phosphoproteomics reveals new PP2A-Cdc55-regulated processes in budding yeast. Gigascience 7:giy047. https://doi.org/10.1093/gigascience/giy047.
32. Tripodi F, Nicastro R, Reghellin V, Coccetti P. 2015. Post-translational modifications on yeast carbon metabolism: regulatory mechanisms beyond transcriptional control. Biochim Biophys Acta 1850:620–627. https://doi.org/10.1016/j.bbagen.2014.12.010.
33. Chen Y, Nielsen J. 2016. Flux control through protein phosphorylation in yeast. FEMS Yeast Res 16:fow096. https://doi.org/10.1093/femsyr/fow096.
34. Nakazawa N, Sato A, Hosaka M. 2016. TORC1 activity is partially reduced under nitrogen starvation conditions in sake yeast Kyokai no. 7, *Saccharomyces cerevisiae*. J Biosci Bioeng 121:247–252. https://doi.org/10.1016/j.jbiosc.2015.07.002.
35. Oliveira AP, Ludwig C, Picotti P, Kogadeeva M, Aebersold R, Sauer U. 2012. Regulation of yeast central metabolism by enzyme phosphorylation. Mol Syst Biol 8:623. https://doi.org/10.1038/msb.2012.55.
36. Goldstein AL, McCusker JH. 1999. Three new dominant drug resistance cassettes for gene disruption in *Saccharomyces cerevisiae*. Yeast 15:1541–1553. https://doi.org/10.1002/(SICI)1097-0061(199910)15:14<1541::AID-YEA476>3.0.CO;2-K.
37. Janke C, Magiera MM, Rathfelder N, Taxis C, Reber S, Maekawa H, Moreno-Borchart A, Doenges G, Schwob E, Schiebel E, Knop M. 2004. A versatile toolbox for PCR-based tagging of yeast genes: new fluorescent proteins, more markers and promoter substitution cassettes. Yeast 21:947–962. https://doi.org/10.1002/yea.1142.
38. Tanigawa M, Maeda T. 2017. An *in vitro* TORC1 kinase assay that recapitulates the Gtr-independent glutamine-responsive TORC1 activation mechanism on yeast vacuoles. Mol Cell Biol 37:e00075-17. https://doi.org/10.1128/MCB.00075-17.
39. Sato M, Dhut S, Toda T. 2005. New drug-resistant cassettes for gene disruption and epitope tagging in *Schizosaccharomyces pombe*. Yeast 22:583–591. https://doi.org/10.1002/yea.1233.
40. Fujita M, Yamamoto M. 1998. *S. pombe sck2*+, a second homologue of *S. cerevisiae SCH9* in fission yeast, encodes a putative protein kinase closely related to PKA in function. Curr Genet 33:248–254. https://doi.org/10.1007/s002940050333.
41. Kinoshita N, Ohkura H, Yanagida M. 1990. Distinct, essential roles of type 1 and 2A protein phosphatases in the control of the fission yeast cell division cycle. Cell 63:405–415. https://doi.org/10.1016/0092-8674(90)90173-C.
42. Kinoshita K, Nemoto T, Nabeshima K, Kondoh H, Niwa H, Yanagida M. 1996. The regulatory subunits of fission yeast protein phosphatase 2A (PP2A) affect cell morphogenesis, cell wall synthesis and cytokinesis. Genes Cells 1:29–45. https://doi.org/10.1046/j.1365-2443.1996.02002.x.
43. Watanabe D, Ota T, Nitta F, Akao T, Shimoi H. 2011. Automatic measurement of sake fermentation kinetics using a multi-channel gas monitor system. J Biosci Bioeng 112:54–57. https://doi.org/10.1016/j.jbiosc.2011.03.007.
44. Soga T, Heiger DN. 2000. Amino acid analysis by capillary electrophoresis electrospray ionization mass spectrometry. Anal Chem 72:1236–1241. https://doi.org/10.1021/ac990976y.
45. Sugimoto M, Wong DT, Hirayama A, Soga T, Tomita M. 2010. Capillary electrophoresis mass spectrometry-based saliva metabolomics identi-

fied oral, breast and pancreatic cancer-specific profiles. Metabolomics 6:78–95. https://doi.org/10.1007/s11306-009-0178-y.
46. Kitamoto K, Oda K, Gomi K, Takahashi K. 1990. Construction of uracil and tryptophan auxotrophic mutants from sake yeasts by disruption of *URA3* and *TRP1* genes. Agric Biol Chem 54:2979–2987. https://doi.org/10.1271/bbb1961.54.2979.
47. Nakazawa N, Abe K, Koshika Y, Iwano K. 2010. Cln3 blocks *IME1* transcription and the Ime1-Ume6 interaction to cause the sporulation incompetence in a sake yeast, Kyokai no. 7. J Biosci Bioeng 110:1–7. https://doi.org/10.1016/j.jbiosc.2010.01.006.
48. Chia KH, Fukuda T, Sofyantoro F, Matsuda T, Amai T, Shiozaki K. 2017. Ragulator and GATOR1 complexes promote fission yeast growth by attenuating TOR complex 1 through Rag GTPases. eLIFE 6:e30880. https://doi.org/10.7554/eLife.30880.